

## Effects of Vehicle Heat on Road Surface Temperature of Dry Condition

A. Fujimoto<sup>1</sup>, H. Watanabe<sup>1</sup> and T. Fukuhara<sup>1</sup>

<sup>1</sup> The University of Fukui  
3-9-1 Bunkyo Fukui-city 910-8507, Japan.  
Email: [a.fujimot@anc.anc-d.fukui-u.ac.jp](mailto:a.fujimot@anc.anc-d.fukui-u.ac.jp)

### ABSTRACT

The formulization of the vehicle related heat fluxes; the tire frictional heat flux, the vehicle radiant heat flux and the vehicle sensible heat flux were incorporated in the heat balance of the road surface layer. A numerical simulation using a two-dimensional vehicle heat model was performed to examine the effects of the vehicle related heat fluxes on road surface temperature of dry condition.

The simulation showed the difference in the road surface temperature between the vehicle and non vehicle-passage areas. The former was about 3°C lower than the latter in the daytime, while about 0.2°C higher during commuting time period in the morning. It is concluded that depending on traffic or weather conditions, the thermal effects of the vehicle related heat fluxes on the road surface temperature cannot be disregarded.

**Keywords:** Vehicle heat, snow and ice prediction model, heat balance

### 1. INTRODUCTION

Road administrators have been strongly required to find ways to reduce road administrative expenses associated with the diminution of government budget for winter road management in Japan. In addition, a complicated change of snow and ice (S/I) conditions on a road surface resulted from weather or traffic makes optimum time of mechanical snow removal or spreading of antifreeze agents difficult. Therefore, a technical tool, which can predict the S/I conditions, should be necessary in order to reconcile the saving of road management cost as well as safe traffic in winter.

For this reason, we have been developing a snow and ice prediction model (SIP model) using a heat balance method. The heat balance of the S/I is determined by both internal and external thermal factors. The internal factors include the road structure and the thermal properties of pavement and road foundation materials. The external factors consist of a natural factor and an artificial factor. The former is weather and geographical features and the latter includes antifreeze agents, heat from vehicles and mechanical snow removal.

SIP models based on heat balance have been reported by Sass [1], Shao & Lister [2], Ishikawa et al. [3], Morstad [4], among others. The common feature of these models is that only the natural factor determines the road surface temperature.

Following these studies, Ishikawa et al. [5] and Takahashi et al. [6] reported that radiant heat from the bottom of a vehicle (vehicle radiant heat) significantly affects the heat balance on a road surface. Kinoshita et al. [7] and Fujimoto et al. [8] pointed out that tire frictional heat (heat transfer between tire and road surface) is important in the occurrence of 'black ice' on road surfaces.

Vehicle heat contributions may consist of the tire frictional heat flux,  $S_t$ , the vehicle radiant heat flux,  $R_v$ , and sensible heat flux due to vehicle induced wind velocity (vehicle sensible heat flux,  $S_{va}$ ). Unfortunately there are very few heat balance models that account for the vehicle related heat fluxes, as far as we know.

In this paper, we propose a two-dimensional vehicle heat model and examine the effects of the vehicle related heat fluxes on road surface temperature of dry condition through a numerical simulation.

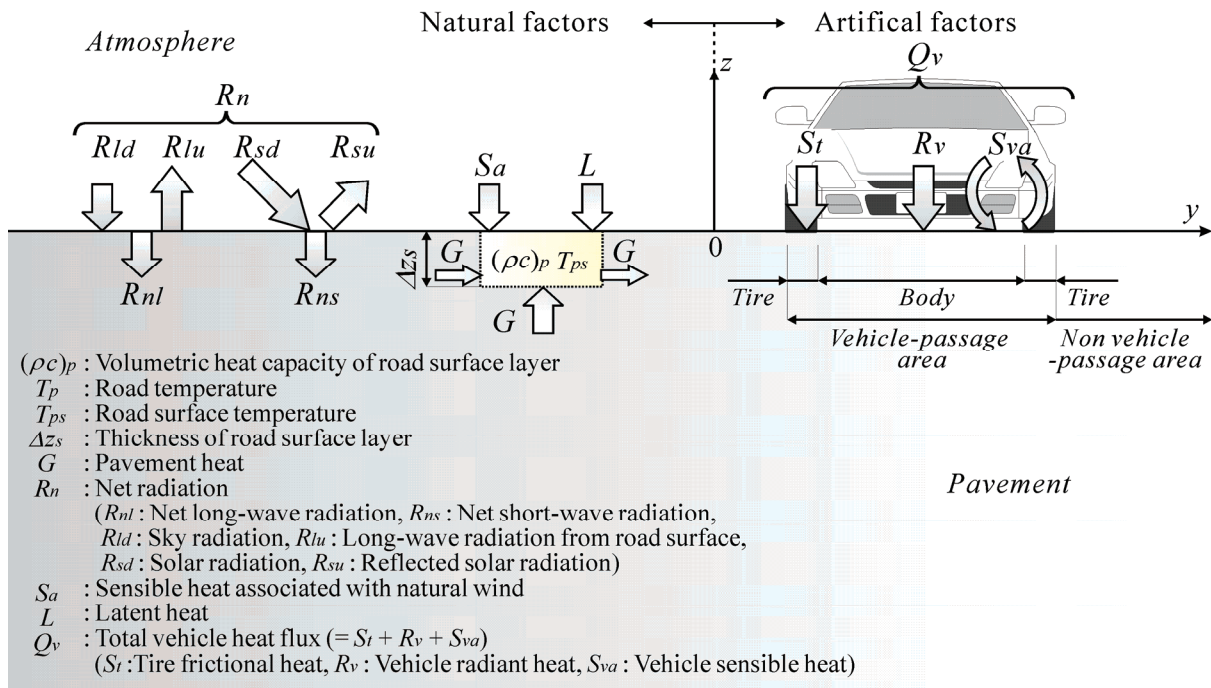


Fig. 1. Schematic view of heat balance of road surface layer including vehicle related heat fluxes.

## 2. HEAT TRANSFER THEORY FOR A DRY ROAD SURFACE

### 2.1 Heat balance equation

Fig. 1 shows the heat balance of a dry road surface layer subjected to the vehicle related heat fluxes. A vehicle-passage area is divided into a vehicle abdomen (inner area between right and left tires) and a tire-passage part. The heat balance of the road surface layer in the tire-passage part is given by Eq. (1):

$$(\rho c)_p \frac{\partial T_{ps}}{\partial t} \Delta z_s = G + R_n + S_a + L + Q_v \quad (1)$$

where  $(\rho c)_p$  is the volumetric heat capacity of the surface layer ( $J/m^3/K$ ),  $t$  is time (s),  $T_{ps}$  is the road surface temperature ( $^\circ C$ ),  $\Delta z_s$  is the thickness of the surface layer (m),  $G$  is the pavement heat flux at the road surface ( $W/m^2$ ),  $R_n$  is the net radiation flux ( $W/m^2$ ),  $S_a$  is the sensible heat flux associated with natural wind ( $W/m^2$ ),  $L$  is the latent heat flux associated with evaporation or condensation ( $W/m^2$ ) and  $Q_v$  is the total vehicle heat flux ( $= S_t + R_v + S_{va}$ ) ( $W/m^2$ ). Supposing that the heat flux in the longitudinal ( $x$ ) direction is very much smaller than that in the transverse ( $y$ ) direction or the vertical ( $z$ ) direction, two dimensional heat transfer analysis becomes appropriate and is adopted in this study. In Fig. 1,  $z = 0$  and  $y = 0$  correspond to the road surface and the center of a road, respectively.

### 2.2 Heat flux components across road surface

#### 2.2.1 Pavement heat flux

Pavement heat flux,  $G$ , is given by the heat conduction equation,

$$G = -\lambda_y \frac{\partial T_p}{\partial y} - \lambda_z \frac{\partial T_p}{\partial z} \Big|_{y=z=0} \quad (2)$$

where  $\lambda_y$  and  $\lambda_z$  are the thermal conductivity of the pavement in the  $y$  and  $z$  directions ( $W/m/K$ ), respectively and  $T_p$  is the road temperature ( $^\circ C$ ). Heat movement in the  $y$  direction is allowable except on the boundary of both sides.

#### 2.2.2 Net radiation flux

Net radiation flux,  $R_n$ , is the sum of the net long-wave radiation flux,  $R_{nl}$  ( $= R_{ld} - R_{lu}$ ), and the net short-wave radiation flux,  $R_{ns}$  ( $= R_{sd} - R_{su}$ ), as shown in Fig. 1. In which,  $R_{lu}$  is the upward long-wave radiation flux from the road surface,  $R_{ld}$  is the downward long-wave radiation flux from the sky,  $R_{sd}$  is the incoming short-wave radiation flux and  $R_{su}$  is the portion reflected upward. Thus,

$$R_n = R_{nl} + R_{ns} = R_{ld} - R_{lu} + R_{sd} - R_{su} \quad (3)$$

where  $R_{lu}$  is calculated according to the Stefan-Boltzmann law,

$$R_{lu} = \varepsilon_p \sigma (T_{ps} + 273.15)^4 \quad (4)$$

where  $\varepsilon_p$  is the emissivity of the road surface (0.95) and  $\sigma$  is the Stefan-Boltzmann constant ( $5.67 \times 10^{-8} \text{ W/m}^2/\text{K}^4$ ).

#### 2.2.3 Sensible heat flux associated with natural wind

Sensible heat flux associated with natural wind,  $S_a$ , is evaluated using Newton's law of cooling,

$$S_a = \alpha_s (T_a - T_{ps}) \quad (5)$$

where  $\alpha_s$  is the heat transfer coefficient between the road surface and atmosphere ( $\text{W/m}^2/\text{K}$ ) and  $T_a$  is atmospheric temperature ( $^\circ\text{C}$ ). The value of  $\alpha_s$  is estimated from the natural wind velocity,  $V_{ws}$  ( $\text{m/s}$ ), using;

$$\alpha_s = 10.4 V_{ws}^{0.7} + 2.2 \quad (6)$$

#### 2.2.4 Latent heat flux

Latent heat flux on the road surface,  $L$ , is expressed as the product of the evaporative or the condensate mass flux,  $m_v$ , and the latent heat of vaporization,  $h_v$ . The value of  $m_v$  may be proportional to the difference in vapor density between road surface and atmosphere. Consequently  $L$  is calculated by the following equation,

$$L = h_v m_v = h_v \alpha_m (\rho_{va} - \rho_{vs}) \quad (7)$$

where  $\alpha_m$  is the vapor transfer coefficient ( $\text{m/s}$ ) and  $\rho_v$  is the density of water vapor ( $\text{kg/m}^3$ ). Subscripts  $a$  and  $s$  refer to air and road surface, respectively.  $\alpha_m$  is calculated in terms of  $V_{ws}$ ,

$$\alpha_m = 1.2 \times 10^{-2} V_{ws}^{0.6} + 0.4 \times 10^{-2} \quad (8)$$

#### 2.2.5 Vehicle related heat fluxes

Total vehicle heat flux,  $Q_v$ , is given by the sum of the tire frictional heat flux,  $S_t$ , the vehicle radiant heat flux,  $R_v$ , and the vehicle sensible heat flux,  $S_{va}$ .

$$Q_v = S_t + R_v + S_{va} \quad (9)$$

$S_t$  may be calculated by Newton's law of cooling,

$$S_t = \alpha_{tp} (T_t - T_{ps}) \quad (10)$$

where  $\alpha_{tp}$  ( $=60 \text{ W/m}^2/\text{K}$ )<sup>[8]</sup> is the heat transfer coefficient between tire and road surface and  $T_t$  is tire temperature ( $^\circ\text{C}$ ).  $T_t$  is given by the following empirical correlation, regardless of road surface conditions (see Fig. 2).

$$T_t = 0.9 T_a + 0.33 V_v \quad (11)$$

where  $V_v$  is vehicle speed ( $\text{km/h}$ ).

$R_v$  may be evaluated by the Stefan-Boltzmann law using the temperature,  $T_v$ , on the bottom surface of the vehicle. That is

$$R_v = \varepsilon_v \sigma (T_v + 273.15)^4 \quad (12)$$

where  $\varepsilon_v$  is the emissivity of steel ( $=0.80$ ).

The spatial variation of  $T_v$  in the  $x$  direction is simplified as shown in Fig. 3. That is

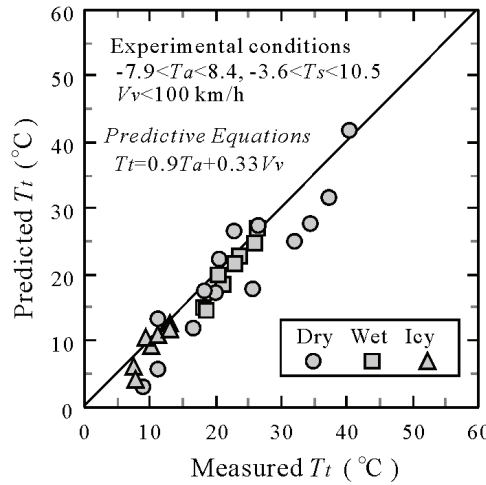


Fig. 2. Correlation of predicted and measured tire temperatures.

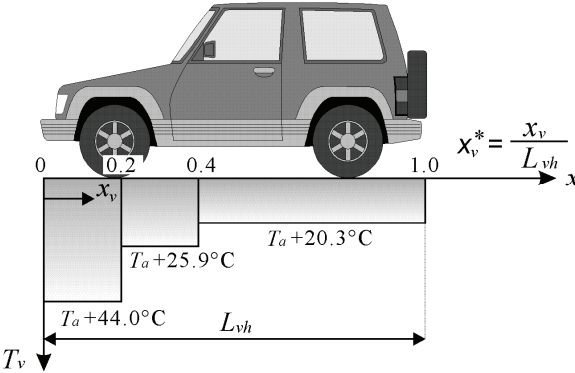


Fig. 3. Spatial variation of temperature of bottom surface of vehicle in  $x$  direction.

$$\begin{aligned} T_v &= T_a + 44.0 & (0 \leq x_v^* \leq 0.2) \\ T_v &= T_a + 25.9 & (0.2 \leq x_v^* \leq 0.4) \\ T_v &= T_a + 20.3 & (0.4 \leq x_v^* \leq 1.0) \end{aligned} \quad (13)$$

where  $x_v^*$  is the normalized distance ( $=x_v/L_{vh}$ ,  $L_{vh}$ : vehicle length,  $x_v$ : distance from the vehicle front).

$S_{va}$  is given by Newton's law of cooling as

$$S_{va} = \alpha_s (T_a - T_{ps}) \quad (14)$$

In this case, in order to calculate  $\alpha_s$ , the vehicle induced wind velocity,  $V_w$  (m/s) is used instead of  $V_{ws}$  in Eq. (6).

Fig. 4 shows the time variation of  $V_w$  for different vehicle speeds,  $V_v$ . During acceleration

$$V_w = at \quad (0 \leq t \leq t_{vmax}) \quad (15)$$

where  $t_{vmax}$  is elapsed time when  $V_w$  reaches a maximum,  $V_{wmax}$ .

For the deceleration period

$$V_w = V_{wmax} \exp\{-b(t - t_{vmax})\} - c(t - t_{vmax}) \quad (t_{vmax} \leq t \leq t_{v0}) \quad (16)$$

where  $t_{v0}$  is elapsed time when  $V_w$  becomes zero again. Coefficients,  $a$ ,  $b$ ,  $c$  and the parameters,  $V_{wmax}$ ,  $t_{vmax}$  and  $t_{v0}$  in Eqs. (15) and (16) are given by the following functions of  $V_v$ , respectively.

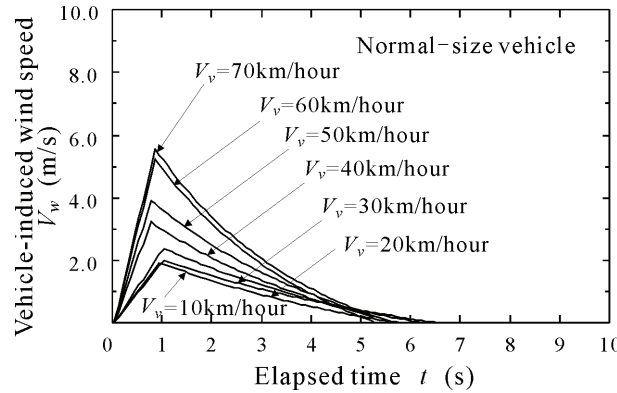


Fig. 4. Time variation of vehicle-induced wind velocity,  $V_w$ , for different vehicle speeds,  $V_v$ .

$$a = 0.08V_v \quad (17)$$

$$b = 0.28 \times 10^{-2}V_v + 0.13 \quad (18)$$

$$c = V_{wmax} \exp\{-b(t_{v0} - t_{vmax})\}/(t_{v0} - t_{vmax}) \quad (19)$$

$$V_{wmax} = 0.08V_v \quad (20)$$

$$t_{vmax} = 1.2 \exp(-0.3 \times 10^{-2}V_v) \quad (21)$$

$$t_{v0} = -1.4 \times 10^{-2}V_v + 7.6 \quad (22)$$

### 3. EVALUATION OF VEHICLE HEAT

#### 3.1 Model assumptions

The vehicle model includes the following assumptions;

- (1) The frequency of vehicle passage is constant and is calculated from hourly traffic volume.
- (2) Road and ground temperatures are uniform in the  $x$  direction.
- (3) Vehicles all pass over the same track within a lane.
- (4) All vehicles are the cars with a standard size ( $L_{vh} = 4.0\text{m}$ ).

#### 3.2 Analytical conditions

This analysis was performed using the weather and traffic data obtained from the observation station (altitude : about 500m) on the route 18 in Myoko city, Niigata, Japan. The data were collected at intervals of 10 minutes from 0:00 on December 25, 2004 for 24 hours. During this period, the weather was fine and the road surface was dry.

The analysis domain is 5.6m in the  $y$  direction and 5.5m in the  $z$  direction. The boundary conditions are (i) the ground temperature is constant along the bottom boundary, and (ii) there is no heat flux across both the side boundaries. The initial vertical temperature profile is given from the data measured at the field observation site. It is supposed that the initial temperature is uniform in the  $y$  direction.

Table 1 shows thermal properties of the pavement and foundation used in this analysis [9].

External conditions required for the present simulation are shown in Figs. 5 and 6. Fig. 5 shows the diurnal variations of the atmospheric temperature,  $T_a$ , relative humidity,  $RH_a$ , and  $V_{ws}$ .

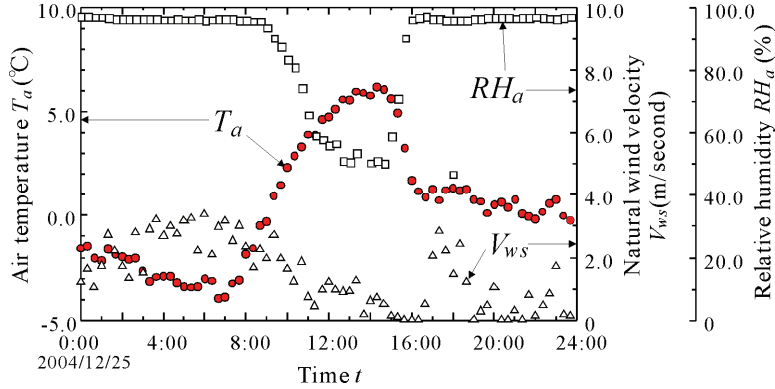
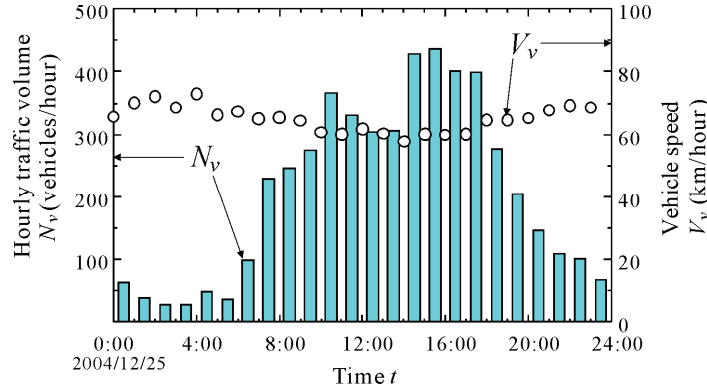
Fig. 6 shows the diurnal variations of the hourly traffic volume,  $N_v$  and hourly averaged speed of vehicle,  $V_v$ .  $V_v$  ranged between 60 and 80km/h and the maximum  $N_v$  was about 450.

#### 3.3 Thermal effects of vehicles

Fig. 7 shows the diurnal variations of the ratio ( $P$ ) of each vehicle related heat flux ( $R_v$  or  $S_i$  or  $S_{va}$ ) to total heat flux across the road surface,  $Q_a$  ( $=|G|+|R_{ns}|+|R_{nl}|+|S_a|+|L|+|R_v|+|S_i|+|S_{va}|$ ), where  $| |$  means an absolute value. The value of  $P$  is given by the following equation.

Table 1. Thermal properties of the pavement and foundation.

Layer	Depth (Thickness) (m)	Density (kg/m <sup>3</sup> )	Specific heat (J/g/K)	Thermal conductivity (W/m/K)
Asphalt	0 – 0.1 (0.1)	2.3	0.9	1.4
Roadbed	0.1 – 0.5 (0.4)	2.0	1.03 [9]	1.8 [9]
Ground	0.5 – 5.6 (5.1)	2.0 [9]	1.6 [9]	1.6 [9]

Fig. 5. Diurnal variations of atmospheric temperature,  $T_a$ , relative humidity,  $RH_a$ , and natural wind velocity,  $V_{ws}$ .Fig. 6. Diurnal variations of hourly traffic volume,  $N_v$  and average speed,  $V_v$ .

$$P = \frac{|R_v| \text{ or } |S_t| \text{ or } |S_{va}|}{|G| + |R_{ns}| + |R_{nl}| + |S_a| + |L| + |R_v| + |S_t| + |S_{va}|} = \frac{|R_v| \text{ or } |S_t| \text{ or } |S_{va}|}{Q_a} \quad (23)$$

$P_{Rv}$  ( $=|R_v|/Q_a$ ) was about 2% in the daytime or nighttime when  $N_v$  is negligible small.  $P_{Rv}$ , however, became 4 to 8% around 8:00 and 16:00 corresponding to time of heavy traffic or low solar radiation.  $P_{St}$  ( $=|S_t|/Q_a$ ) had in general the same pattern as  $P_{Rv}$  but was always smaller than  $P_{Rv}$ .  $P_{Sva}$  ( $=|S_{va}|/Q_a$ ) was less than 1% between 0:00 and 7:00. Subsequently  $P_{Sva}$  increased as the solar radiation,  $R_{sd}$ , and temperature difference,  $\Delta T_{pa}$ , between the atmosphere and road surface increased, and reached 20% at the maximum at 16:00. The remarkable fall of  $P_{Sva}$  at 17:00 was caused by the decrease of  $\Delta T_{pa}$ . Subsequently, the sum of  $P_{St}$  and  $P_{Rv}$  reached 8 to 10% between 18:00 and 19:00.

### 3.4 Road surface temperature

#### 3.4.1 Characteristics of time variation

Fig. 8 shows the diurnal variations of  $T_{ps}$  in the non vehicle-passage area where is 1.5m away from the tire-passage part in the y direction ( $3.4 \leq y \leq 3.6\text{m}$ ). The symbol (○) and solid line in Fig. 8 are the measured and

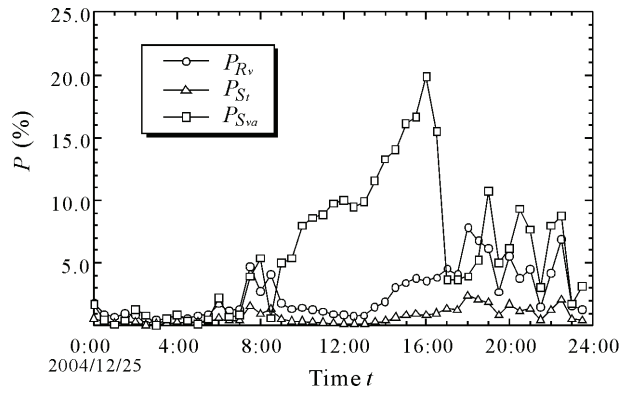


Fig. 7. Diurnal variations of ratio of vehicle related heat fluxes to total heat flux across road surface.

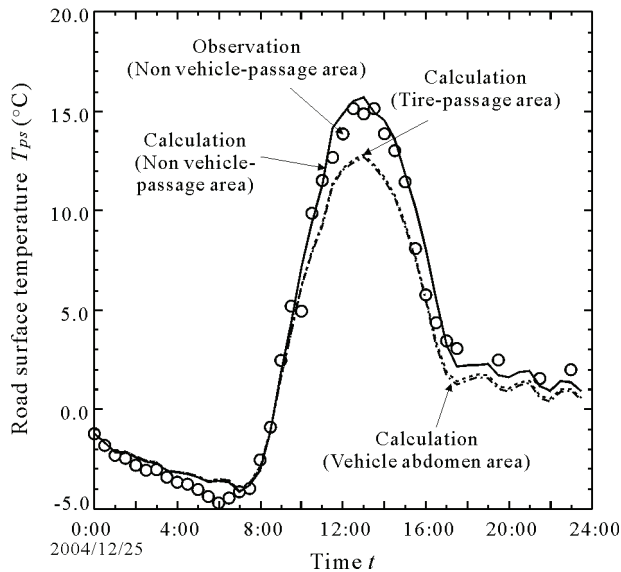


Fig. 8. Diurnal variations of road surface temperature,  $T_{ps}$ .

calculated values, respectively. Both results were in good agreement. A dashed line and a dashed and single-dotted one represent the calculated value of  $T_{ps}$  in the tire-passage part and in the vehicle abdomen area, respectively. The difference between these two lines is very small at any time. It can be guessed that the tire frictional heat is negligible as long as this traffic condition is concerned.

Comparing  $T_{ps}$  in the vehicle-passage area with  $T_{ps}$  in the non vehicle-passage area, it was found that the former was about 3°C lower than the latter in the daytime. This is attributed to the vehicle sensible heat and shielding effect of a vehicle on the solar radiation and downward sky radiation. This temperature difference, however, decreased to about 0.5°C after sunset and finally disappeared in the midnight.

### 3.4.2 Characteristics of transversal profile

Fig. 9 shows the diurnal variations of the transversal profile of  $T_{ps}$  in the range of 1.0m to 4.5m away from the center of a road. The gray in the figure shows the vehicle passage area (thin gray: the vehicle abdomen area, deep gray: the tire-passage part). As described above,  $T_{ps}$  in the vehicle passage area is about 3°C lower than  $T_{ps}$  in the non vehicle-passage area at 12:00. Inversely,  $T_{ps}$  in the tire-passage part became 0.2°C relatively higher than  $T_{ps}$  in the non vehicle-passage area at 8:00 associated with  $S_t$ .

## 4. CONCLUSIONS

The formulation of the vehicle related heat fluxes; the tire frictional heat flux,  $S_t$ , the vehicle radiant heat flux,  $R_v$ , and vehicle sensible heat flux,  $S_{va}$ , were incorporated in the heat balance of the road surface layer.

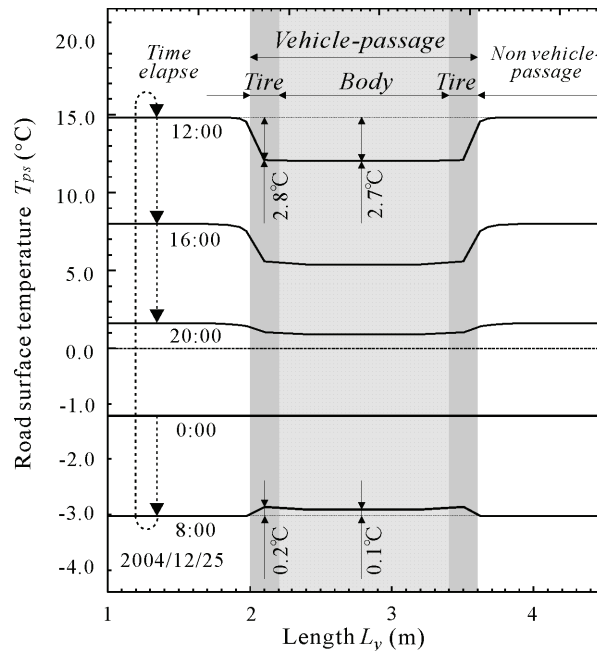


Fig. 9. Diurnal variations of the transversal profile of road surface temperature.

The simulation could show how the road surface temperature would be changed by traffic and weather conditions. The ratio of the sum of  $S_t$  and  $R_v$  to the total heat flux,  $Q_a$ , across the road surface reached 8 to 10% between 18:00 and 19:00, and the ratio of  $S_{va}$  to  $Q_a$  reached about 20% at the maximum. The simulation also showed the difference in the road surface temperature,  $T_{ps}$ , between the vehicle and non vehicle-passage areas. For example, the former was about 3°C lower than the latter in the daytime, while about 0.2°C higher during commuting time period in the morning. It is concluded that depending on traffic or weather conditions, the thermal effects of the vehicle related heat fluxes on melting or re-freezing of snow/ice on a road cannot be disregarded.

## 5. REFERENCES

- [1] Sass, B.H. 1992. A numerical model for prediction road temperature and ice. *The Journal of Applied Meteorology*, 31 : 1499-1506.
- [2] Shao, J. & Lister, P.J. 1996. An automated nowcasting model of road surface temperature and state for winter road maintenance. *The Journal of Applied Meteorology*, 35 : 1352-1361.
- [3] Ishikawa, N., Naruse, R. & Maeno, N. 1987. Heat balance characteristics of road snow, *Low temperature science. Ser. A, Physical sciences*, 46: 151-162.
- [4] Morstad, B., Adams, E.E., McKittrick, L.R. & Bristow, J.R. 2004. Thermal model for contaminated snow on pavement, *Proceedings of the Fifth International Conference on Snow Engineering*, 5 : 33-38.
- [5] Ishikawa, N., Narita, H. & Kajiya, Y. 2000. Heat balance characteristics of snow melting on roads, *Proceedings of cold region technology conference*, 16: 382-388.
- [6] Takahashi, N., Asano, M. & Ishikawa, N. 2005. Developing a method to predict road surface icing conditions applying a heat balance method, *Proceedings of cold region technology conference*, 21: 201-208.
- [7] Kinoshita, S., Akitaya, E. & Tanuma, K. 1970. Snow and ice on roads. II., *Low temperature science. Ser. A, Physical sciences*, 28: 311-323.
- [8] Fujimoto, A., Watanabe, H. & Fukuhara, T. 2006. Effects of tire frictional heat on snow covered surface, *Standing international road weather conference*, 13: 117-122.
- [9] Japan society of mechanical engineers. 1983. Heat transfer handbook: 238 and 375.

## ACKNOWLEDGEMENT

Gratitude is expressed to data offer for this simulation from the Public Works Research Institute Niigata experiment station.